

Application of Intrinsic Time-Scale Decomposition in Ground Penetrating Radar Data Processing

Yunwei Zhao *, Wen Zeng, Lingxing Peng, Pengtao Zhao, Dexuan Li

Hunan Provincial communications planning, survey&design institute co., LTD., Changsha Hunan, 410200, China

* Corresponding author: Yunwei Zhao (Email: zhaoyunwei2008@126.com)

Abstract: In order to improve the accuracy of Ground Penetrating Radar image analysis and interpretation, to realize the effective detection of tunnel structure, as well as to improve the performance of its application in engineering inspection, this study adopts the intrinsic time-scale decomposition method to process the Ground Penetrating Radar data. By analyzing the processed data, we find that this method has significant effect in improving the accuracy and stability of Ground Penetrating Radar data processing, and this study is of great significance for the practical application of Ground Penetrating Radar.

Keywords: Intrinsic Time-scale Decomposition; Ground Penetrating Radar; Data Processing.

1. Introduction

In recent years, Ground Penetrating Radar (GPR) technology, as a very effective non-destructive testing (NDT) tool, has been widely used in the detection and analysis of tunnel structures. However, processing and interpreting Ground Penetrating Radar data have been a challenging task due to its complex waveform characteristics and noise interference. Therefore, improving the analysis and interpretation of Ground Penetrating Radar images has been a challenge in the field of Ground Penetrating Radar.

In the past decades, the Intrinsic Time-Scale Decomposition (ITD) has been widely used in the field of signal processing with remarkable results. The method has emerged as a powerful nonlinear and non-stationary signal analysis technique, addressing limitations inherent in classical methods such as the Fourier and wavelet transforms (Frei and Osorio, 2007). This approach facilitates efficient time-frequency-energy (TFE) analysis, enabling the extracting of meaningful features from complex signals. Its capability to decipher minute changes in signals makes it particularly suitable for applications involving nonlinear-signal data processing, such as EEG analysis for seizure prediction (Martis et al., 2013) and fault diagnosis in mechanical systems (An et al., 2012; Jin et al., 2017).

Several studies have demonstrated the versatility of ITD in practical fault diagnosis scenarios. For instance, (Hu et al., 2015) introduced an ensemble version of ITD (EITD), which employs cubic spline interpolation and linear transformation to mitigate end effects and signal distortion, thereby enhancing fault detection accuracy in wind turbine gearboxes. Similarly, Zhang and Liu (2017) combined complete ensemble ITD (CEITD) with least-square support vector machines (LSSVM), optimized via hybrid algorithms, to effectively identify faults in diesel engines, overcoming mode-mixing issues typical of standard ITD.

The application of ITD extends to the analysis of vibration signals for gear and planetary gearbox fault diagnosis under variable conditions. (Xing et al., 2017) Integrated ITD with singular value decomposition (SVD) and SVM to improve fault classification robustness. (Feng et al., 2016) utilized joint amplitude and frequency demodulation based on ITD to

address multiple modulation sources in planetary gearboxes, further validating the method through experimental signals.

In biomedical signal processing, ITD has been employed for automated seizure prediction from EEG signals, where it enables the extraction of subtle nonlinear features critical for classification tasks (Martis et al., 2013). Additionally, Jin et al. (2017) developed an automated quantification method for fragmented QRS complexes, leveraging ITD to provide objective and efficient analysis compared to traditional visual inspection.

The adaptability of ITD to various domains is further exemplified by its application in identifying specific emitter signals, such as communication and radar signals, where it aids in estimating instantaneous parameters for emitter recognition (Song et al., 2010). Moreover, the method's potential in environmental monitoring has been explored, with (Rezaie-Balf et al., 2020) applying an ensemble Kalman filter combined with neural networks for water quality index prediction, illustrating the broader applicability of data-driven models integrated with ITD.

Overall, the literature underscores ITD's effectiveness in extracting meaningful features from complex, nonlinear, and non-stationary signals across diverse fields, including mechanical fault diagnosis, biomedical signal analysis, and environmental monitoring.

The aim of this study is to explore the application of the intrinsic time-scale decomposition in the processing of Ground Penetrating Radar data and to further improve the analysis and interpretation of Ground Penetrating Radar images, which can be used to effectively detect the tunnel structure and obtain important structural information through the intrinsic time-scale decomposition of Ground Penetrating Radar data.

2. The Intrinsic Time-scale Decomposition

Intrinsic Time-Scale Decomposition (ITD) was proposed by Mark G. Frei and Ivan Osorio in 2007. The purpose of ITD is to decompose the data into a series of intrinsic rotational components that characterize the signal and a monotonic trend component. The ITD algorithm employs a single-wave analysis, which is capable of real-time processing of signals

and provides an efficient and accurate time-frequency analysis method in the field of signal analysis. The ITD algorithm uses a single-wave analysis method to process the signal in real time, providing an efficient and accurate time-frequency analysis method for signal analysis.

Assume X_t is the original signal, and define L as the baseline extraction operator. After applying L to the original signal, the remaining residual is defined as the intrinsic rotation. Thus, if the intrinsic rotation extraction operator is denoted by H , then $H=1-L$. This yields a one-step decomposition of X_t as:

$$X_t = LX_t + (1-L)X_t = L_t + H_t \quad (1)$$

$$L_{k+1} = \alpha \left[x_k + \left(\frac{\tau_{k+1} - \tau_k}{\tau_{k+2} - \tau_k} \right) (x_{k+2} - x_k) \right] + (1-\alpha)x_{k+1} \quad (3)$$

The value of α is (0, 1), usually 0.5, but in practice, with the change of the signal, the value is not necessarily the best to take 0.5. In general, for high-frequency components of the signal, the value of α should be slightly larger, while for low-frequency components of the signal, the value should be slightly smaller. But in general, it is better to take a value between 0.4 and 0.6.

For each decomposition, the resulting base signal is reused as the input signal to continue the decomposition until a monotonic signal is obtained. This decomposes the original signal into a series of sums of intrinsic rotational components of decreasing instantaneous frequency and a monotonic trend component.

$$\begin{aligned} X_t &= Hx_t + Lx_t \\ &= Hx_t + (H+L)Lx_t \\ &= (H(1+L) + L^2)x_t \\ &= \left(H \sum_{k=0}^{p-1} L^k + L^p \right) x_t \end{aligned} \quad (4)$$

where $HL^k x_t$ is the $(k+1)$ st level proper rotation signal and $L^p x_t$ is either the monotonic trend or the lowest frequency baseline extracted if the decomposition is stopped before the monotonic trend is reached. Here, $H=1-L$ is used, and the formula for telescoping summation is as follows:

$$1 - L^p = (1-L)(1+L+\dots+L^{p-2}+L^{p-1}) \quad (5)$$

The steps of one ITD decomposition are as follows:

(1) The extreme points $\{\tau_k, k=1,2,\dots\}$ of the original signal (green solid line) change in real time with the signal. the ITD method waits for the next local extreme point based on the current local extreme point, after which it proceeds to the next step.

(2) New extreme points of the original signal are quickly detected, and monotonic fragments of the baseline are constructed in the adjacent interval of extreme points.

(3) The baseline signal fragment is restricted to the already described starting and ending intervals when it is in the interval of extreme value points, and can be linearly transformed to the input signal.

(4) The original signal is subtracted from the baseline signal to produce the rotational component at high frequencies, and then the decomposition is continued by using the above baseline signal as the new channel input signal.

where L_t is the baseline signal, representing the relatively low-frequency portions. H_t is the proper rotational signal, representing the relative high-frequency portions.

Let $\{\tau_k, k=1,2,\dots\}$ be the extreme points of the signal $\{x_t, t > 0\}$ and for convenience define $\tau_0=0$. Denote $X(\tau_k)$ and $L(\tau_k)$ by X_k and L_k , respectively, and assume that L_t and H_t are defined on $[0, \tau_k]$ and that X_t makes sense on $[0, \tau_{k+2}]$. L is the baseline extraction operator defined on $(\tau_k, \tau_{k+1}]$:

$$L_{x_t} = L_t = L_k + \left(\frac{L_{k+1} - L_k}{x_{k+1} - x_k} \right) (x_t - x_k) \quad (2)$$

where,

(5) Repeat the decomposition using the above method, the original signal will be decomposed into a series of rotational components and a trend component, each rotational signal according to the frequency band from high to low to decompose the obtained, so the ITD algorithm this method of signal analysis is adaptive, can be used for the analysis of non-smooth and nonlinear signals.

3. Application of Intrinsic Time-scaled Decomposition to GPR

The limitations of conventional ground-penetrating radar (GPR) data processing are well-documented across multiple studies, highlighting challenges in resolution, spatiotemporal dynamics, noise suppression, and data interpretation. Traditional GPR techniques often struggle to accurately resolve subsurface features due to inherent methodological constraints. One prominent limitation pertains to resolution. (Langman et al., 1994) demonstrated that the performance of GPR systems, especially when employing the extended Prony method, is significantly affected by the signal-to-noise ratio (SNR).

In order to verify the effectiveness of the intrinsic time-scale decomposition in improving the effect of ground-penetrating radar data processing, this study selects the ground-penetrating radar raw data of two typical tunnel secondary lining deholloving diseases, and through the step-by-step decomposition of the raw data, the signal is decomposed into a series of PRC components, and the signal and the noise are distributed in these components according to their own instantaneous frequency spectrum characteristics, and the components where the signal is located are superimposed through the reconstruction, thus removing the noise contained in the signal.

Fig. 1 shows a typical deholloving disease of the tunnel secondary lining structure, which mainly appears at the intersection of two secondary linings, and the shape of this disease is manifested as a triangle, Figure 1(a) is the result of comparing the original waveform of the 350th data (scan is 350) and the waveform of the data processed based on the intrinsic time scale decomposition method, and Figure 1(b) is the relative error of the two waveforms in Fig. 1(a), which is calculated as follows

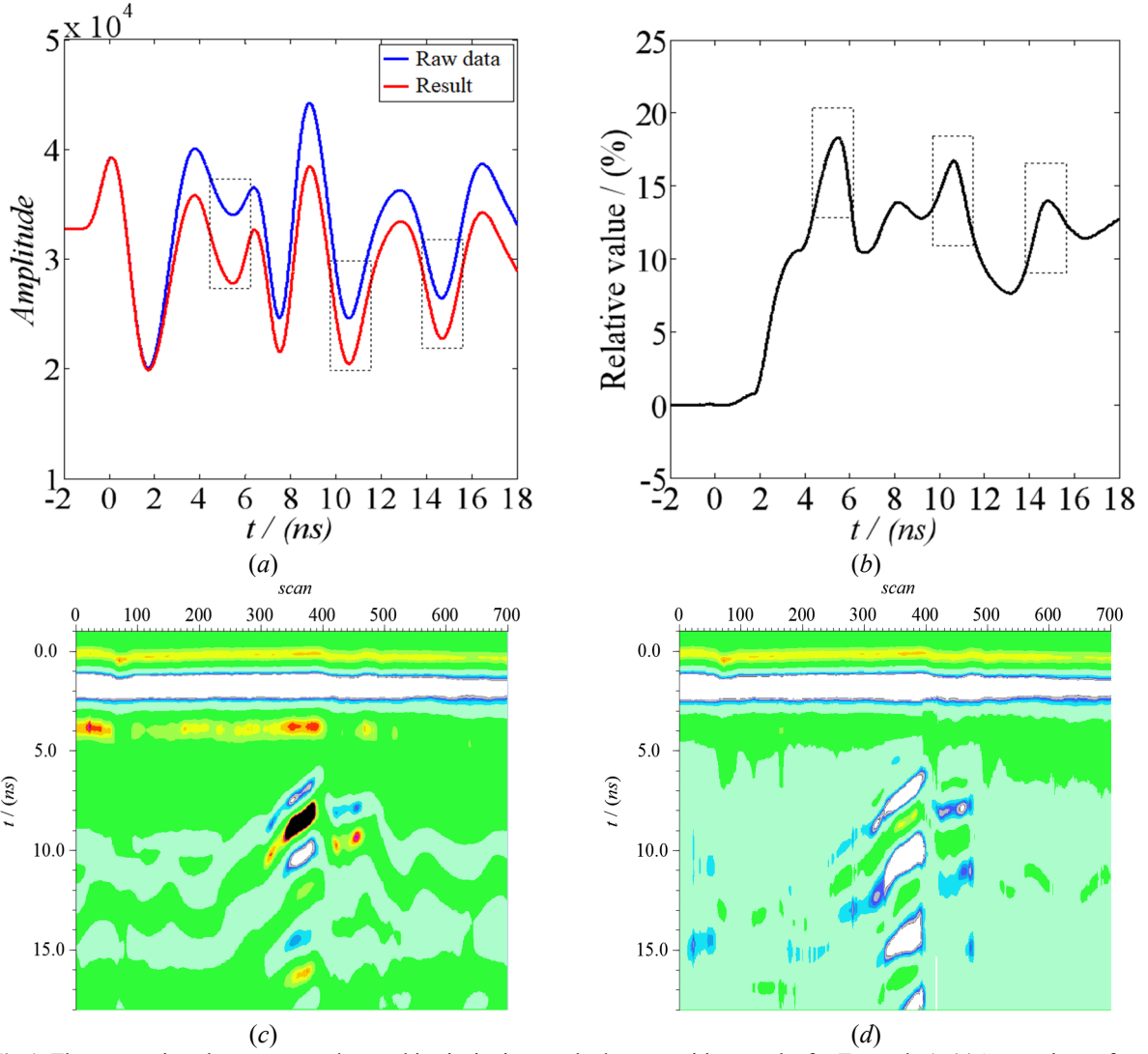


Fig 1. The comparison between raw data and intrinsic time-scale decomposition results for Example 1. (a) Comparison of wave for scan=350, (b) The relative error for scan=350, (c) Raw Data, (d) The results of intrinsic time-scale decomposition

$$R = \left| \frac{d_{result} - d_{raw}}{d_{raw}} \right| \times 100\% \quad (6)$$

where R is the relative error, d_{result} is the processing result based on the intrinsic time-scale decomposition, and d_{raw} is the original data.

From Fig. 1(b), it can be seen that there are four obvious positive extreme points of the relative error, t is $5.5ns$, $8.1ns$, $10.6ns$, $14.8ns$, respectively, and correspondingly, its relative error is 18.28% , 13.84% , 16.71% , 13.98% , respectively. When t is $5.5ns$, the waveform is the reflected wave at the upper interface of the debonding lesion; when t is $8.1ns$, the waveform is the reflected wave at the lower interface of the debonding lesion; and when t is $10.6ns$ and t is $14.8ns$, the waveform is the multiple reflected wave of the debonding lesion. As can be seen from Fig. 1(b) and Fig. 1(d), after the treatment of the intrinsic time scale decomposition, the amplitudes of the reflected waves at the upper and lower interfaces of the disease are significantly improved, which are easier to recognize. At the same time, the multiple reflected wave amplitude of the infestation is also increased and is unsuppressed.

Fig. 2 shows a conventional deholing disease of the tunnel secondary lining structure, which exhibits a horizontal shape. Fig. 2(a) shows the results of the comparison between

the original waveform of the 350th data (scan is 350) and the waveform of the data processed based on the intrinsic time-scale decomposition, and Fig. 2(b) shows the relative errors of the two waveforms in Fig. 2(a).

From Fig. 2(b), it can be seen that there are four obvious positive extreme points of the relative errors, t is $4.9ns$, $6.6ns$, $9.7ns$, $11.1ns$, and correspondingly, their relative errors are 18.46% , 13.82% , 17.18% , 15.76% , respectively. When t is $4.9ns$, the waveform is the reflected wave at the upper interface of the debonding lesion; when t is $6.6ns$, the waveform is the reflected wave at the lower interface of the debonding lesion; and when t is $9.7ns$ and t is $11.1ns$, the waveform is the multiple reflected wave of the debonding lesion. As can be seen from Fig. 2(b) and Fig. 2(d), after the treatment of the intrinsic time-scale decomposition, the amplitudes of the reflected waves at the upper and lower interfaces of the disease are significantly improved, which are easier to recognize. At the same time, the multiple reflected wave amplitude of the infestation is also increased and is unsuppressed.

As can be seen from Figs. 1 and 2, after the processing of the raw data by the intrinsic time-scale decomposition, the reflected waves at the upper and lower interfaces of the disease are amplified and more easily recognized. At the same time, its multiple reflected waves are also amplified, and the

intrinsic time scale method cannot suppress the multiple reflected waves.

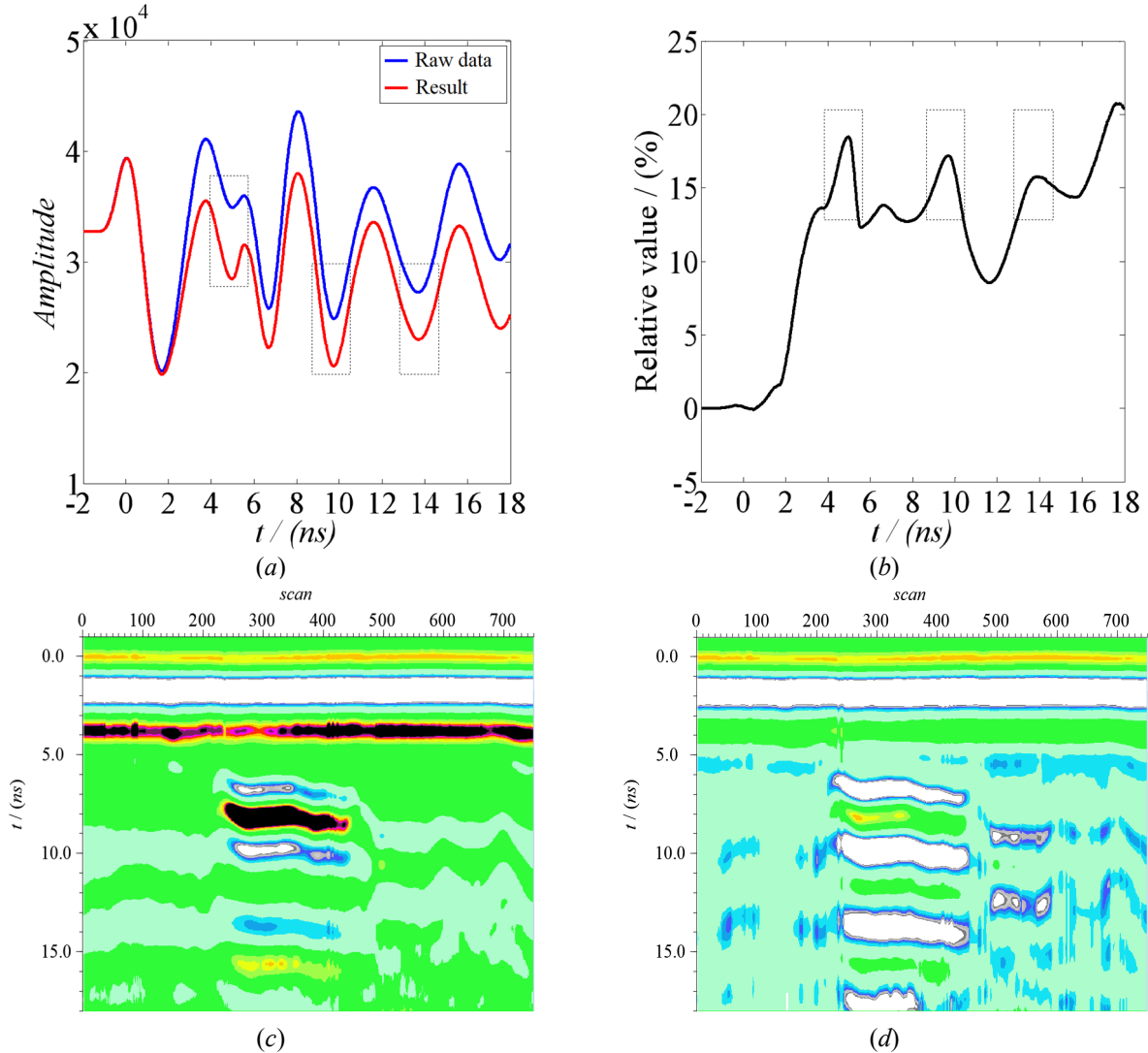


Fig 2. The comparison between raw data and intrinsic time-scale decomposition results for Example 2. (a)Comparison of wave for scan=350,(b)The relative error for scan=350, (c) Raw Data, (d) The results of intrinsic time-scale decomposition

4. Conclusion

In this study, by exploring the application of the intrinsic time-scale decomposition in ground penetrating radar data processing, effective detection of tunnel structures is realized, and important structural information is obtained.

(1) This method has an obvious effect in improving the analysis and interpretation of ground penetrating radar images. Compared with the traditional ground penetrating radar data processing methods, this method presents significant advantages in improving the processing accuracy and stability.

(2) There are still some shortcomings in this study that need to be further improved. The applicability and feasibility of the intrinsic time-scale decomposition in ground penetrating radar data processing need to be further verified, especially the stability and reliability under different geological environments and radar parameter settings. The data processing methods and parameter settings in this study need to be optimized to achieve more accurate and reproducible ground penetrating radar data processing results.

(3) Finally, this study is only limited to the application of the intrinsic time-scale decomposition in ground penetrating radar data processing, and does not involve the comparison

and optimization of other related methods and data processing techniques.

Acknowledgments

The authors would like to thank the anonymous reviewers for their valuable comments and suggestions that helped improve the quality of this manuscript.

References

- [1] An, X., Jiang, D., Chen, J. and Liu, C., 2012. Application of the intrinsic time-scale decomposition method to fault diagnosis of wind turbine bearing. *Journal of vibration and control*, 18(2): 240-245.
- [2] Feng, Z., Lin, X. and Zuo, M.J., 2016. Joint amplitude and frequency demodulation analysis based on intrinsic time-scale decomposition for planetary gearbox fault diagnosis. *Mechanical Systems and Signal Processing*, 72-73: 223-240.
- [3] Frei, M.G. and Osorio, I., 2007. Intrinsic time-scale decomposition: time–frequency–energy analysis and real-time filtering of non-stationary signals. *Proceedings of the Royal Society. A, Mathematical, physical, and engineering sciences*, 463(2078): 321-342.

- [4] Hu, A., Yan, X. and Xiang, L., 2015. A new wind turbine fault diagnosis method based on ensemble intrinsic time-scale decomposition and WPT-fractal dimension. *Renewable Energy*, 83: 767-778.
- [5] Jin, F., Sugavaneswaran, L., Krishnan, S. and Chauhan, V.S., 2017. Quantification of fragmented QRS complex using intrinsic time-scale decomposition. *Biomedical Signal Processing and Control*, 31: 513-523.
- [6] Langman, A., Inggs, M.R. and Flores, B.C., 1994. Improving the resolution of a stepped frequency cw ground-penetrating radar. *SPIE*, pp. 146-155.
- [7] Martis, R.J. et al., 2013. Application of intrinsic time-scale decomposition (ITD) to EEG signals for automated seizure prediction. *Int J Neural Syst*, 23(5): 1350023.
- [8] Rezaie-Balf, M. et al., 2020. Physicochemical parameters data assimilation for efficient improvement of water quality index prediction: Comparative assessment of a noise suppression hybridization approach. *Journal of Cleaner Production*, 271: 122576.
- [9] Song, C., Zhan, Y. and Guo, L., 2010. Specific Emitter Identification Based on Intrinsic Time-Scale Decomposition, 2010 6th International Conference on Wireless Communications Networking and Mobile Computing (WiCOM), pp. 1-4.
- [10] Xing, Z., Qu, J., Chai, Y., Tang, Q. and Zhou, Y., 2017. Gear fault diagnosis under variable conditions with intrinsic time-scale decomposition-singular value decomposition and support vector machine. *Journal of Mechanical Science and Technology*, 31(2): 545-553.
- [11] Zhang, J. and Liu, Y., 2017. Application of complete ensemble intrinsic time-scale decomposition and least-square SVM optimized using hybrid DE and PSO to fault diagnosis of diesel engines. *Frontiers of Information Technology & Electronic Engineering*, 18(2): 272-286.